

CMU-NET: A STRONG CONVMIXER-BASED MEDICAL ULTRASOUND IMAGE SEGMENTATION NETWORK

Fenghe Tang¹, Lingtao Wang¹, Chunping Ning², Min Xian³, and Jianrui Ding^{1*}

¹School of Computer Science and Technology, Harbin Institute of Technology, Harbin, China.

²Ultrasound Department, The Affiliated Hospital of Qingdao University, Qingdao, China.

³Department of Computer Science, University of Idaho, Idaho Falls, ID 83401, USA

ABSTRACT

U-Net and its extended segmentation model have achieved great success in medical image segmentation tasks. However, due to the inherent local characteristics of ordinary convolution operations, the encoder cannot effectively extract the global context information. In addition, simple skip connection cannot capture salient features. In this work, we propose a full convolutional segmentation network (CMU-Net) which incorporate hybrid convolution and multi-scale attention gate. The ConvMixer module is to mix distant spatial locations for extracting the global context information. Moreover, the multi-scale attention gate can help to emphasize valuable features and achieve efficient skip connections. Evaluations on open-source breast ultrasound images and private thyroid ultrasound image datasets show that CMU-Net achieves an average IOU of 73.27% and 84.75%, F1-value is 84.16% and 91.71%. The code is available at <https://github.com/FengheTan9/CMU-Net>.

Index Terms— Ultrasound image segmentation, U-Net, ConvMixer, multi-scale attention

1. INTRODUCTION

Ultrasound imaging technology is a non-invasive, non-radiation, low cost and real time detection method. It has widely used in the detection of breast tumor, thyroid nodule, fetal, and gonadal tissue [1]. Manual localization of lesions is laborious and time-consuming. It also will be affected by subjective factors such as radiologists' experience and mental state, which is prone to misdiagnosis. With the emergence of deep learning technology, automatic medical image segmentation has been rapidly developed in the field of image analysis, which can effectively overcome the above limitations.

As shown in Figure 1, generally, lesion on ultrasound images can be segmented into single target, but its size and shape in different cases vary greatly. In addition, the sample size of medical images is small. These characteristics makes automatic ultrasound medical image segmentation very challenging. U-Net [2] is an encoder-decoder based segmentation net-

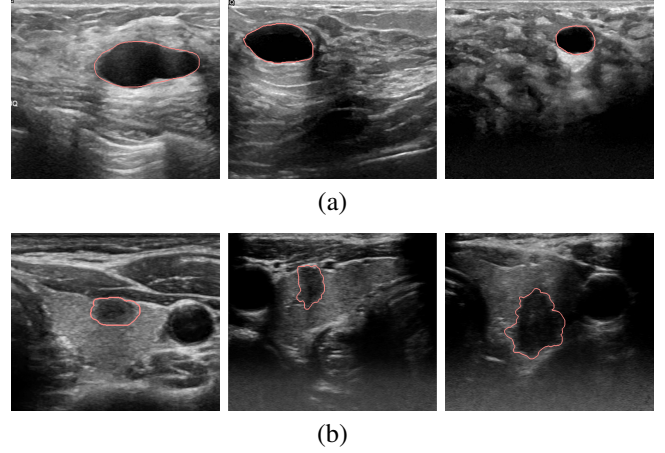


Fig. 1. Examples of ultrasound image segmentation. The pink contour denotes the ultrasound lesion region.(a) breast ultrasound image (b) thyroid ultrasound image

work. It can effectively fit the scarce medical image data. In recent years, a great deal of medical segmentation networks based on U-Net have been proposed, such as U-Net++ [3], Attention U-Net [4], Unet3+ [5], UNeXt [6]. Due to the locality of ordinary convolution operations, a number of networks based on Transformer [7], which can effectively extract the global information of images, have recently been applied for medical image segmentation tasks [8, 9, 10]. TransUnet [8] employs Vit [11] to obtain the global context with CNN, but it requires massive medical images and computing overhead.

In order to solve the limitation of ordinary convolution locality, Trockman proposed the ConvMixer [12]. The ConvMixer uses large convolutional kernels to mix remote spatial locations to obtain global context information. Compared with the Transformer, the ConvMixer which uses convolutional inductive bias is more efficiency and better adapt to computer vision tasks, and its computational overhead is less than that of the self-attention mechanism.

Inspired by the U-shape architectural design and ConvMixer, we propose CMU-Net which is an efficient full convolutional image segmentation network. The ConvMixer module is used to extract global context information. In

addition, multi-scale attention gate is proposed to suppress irrelevant features and strengthen the valuable features. We evaluate CMU-Net on open-source Breast UltraSound Images (BUSI) dataset [13] and private Thyroid UltraSound dataset (TUS). The results show that CMU-Net performs better than the recent and prevalent medical image segmentation models.

This paper makes the following contributions: 1) We propose a strong full convolution medical image segmentation network based on ConvMixer. 2) We propose multi-scale attention gates, which can effectively transfer knowledge in skip-connection. 3) We successfully improved the performance of ultrasound medical image segmentation task.

2. METHOD

Our proposed CMU-Net is shown in Figure 2. We still follow $C1 = 64$, $C2 = 128$, $C3 = 256$, $C4 = 512$, $C5 = 1024$ as usual U-Shape architecture. The CMU-Net is divided into the encoder stage and the decoder stage with skip-connection. In the encoder stage, high-level semantic information of medical images is extracted through ordinary convolution and its feature map as patches are input into the ConvMixer module to obtain mixed spatial and location information. In the decoder stage, the valuable encoder features from multi-scale attention gates are spliced with the corresponding up-sampling features to achieve accurate positioning.

2.1. Encoder stage

The encoder is divided into five levels from top to bottom. Each level consists of two ordinary convolution blocks and a down sampling. Specifically, each ordinary convolution block is equipped with a convolution layer, a batch normalization layer and ReLU activation. The convolution kernel size is 3×3 , stride of 1 and padding of 1. The down sam-

pling of the encoder is max pooling with pool window 2×2 . At the last level, we input the feature map as patches to the ConvMixer block [12]. As shown in Figure 2, the ConvMixer module is composed of the L ConvMixer layers. A single ConvMixer layer consists of depthwise convolution (i.e., kernel size $k \times k$) and pointwise convolution (i.e., kernel size 1×1). The number of group channels of depthwise convolution kernel is equal to the channels of the input feature map. Each convolution is with a GELU [14] activation and a batch normalization as follows:

$$f'_l = BN(\sigma_1\{DepthwiseConv(f_{l-1})\}) + f_{l-1} \quad (1)$$

$$f_l = BN(\sigma_1\{PointwiseConv(f'_l)\}) \quad (2)$$

Where f_l represents the output feature map of layer l in ConvMixer block, σ_1 represents the GeLU activation, BN represents the batch normalization. Since the feature map output from all layers in the ConvMixer module maintain the same resolution and size, we directly up-sampling the features extracted by the ConvMixer block.

2.2. Decoder stage with skip-connection

The decoder is divided into five levels from bottom to top. Each level is composed of two ordinary convolution blocks and a up sampling block. Specifically, up sampling block is equipped with a upsample layer, a convolution layer, a batch normalization layer and ReLU activation. we use bilinear interpolation to upsample the feature maps and the convolution kernel size is 3×3 , stride of 1 and padding of 1.

In skip-connection phase at each level, we propose a multi-scale attention gate, which is used to suppress unimportant encoded features and enhance the valuable features. Specifically, the implementation of multi-scale attention gates is shown in the Figure 3.

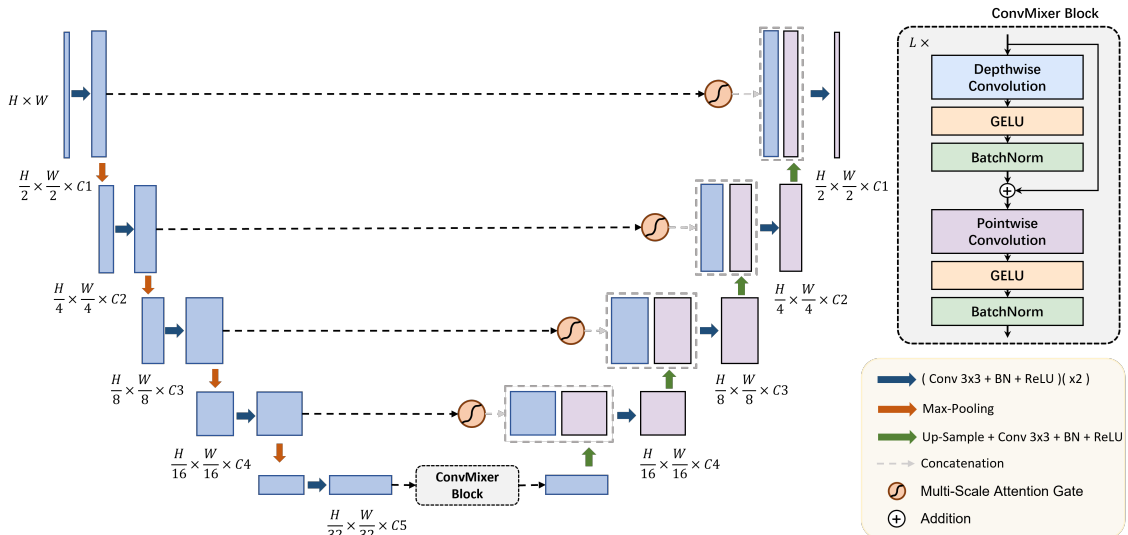


Fig. 2. Overview of the proposed CMU-Net architecture.

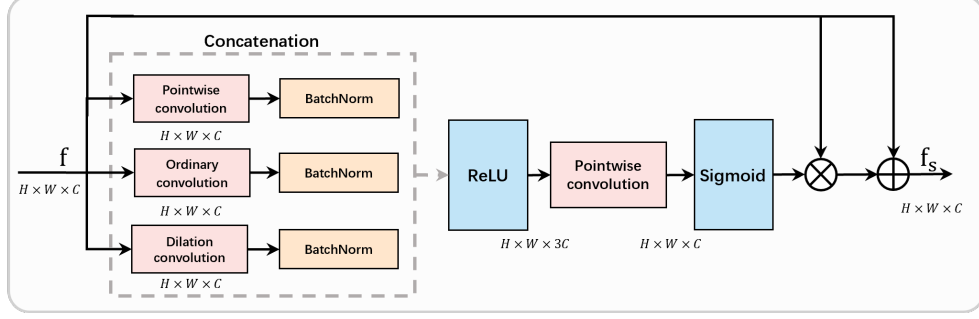


Fig. 3. Multi-scale attention gate

In order to select encoder features according to different resolutions adaptively, we deploy three convolutions with different receptive field to extract features: pointwise convolution, ordinary convolution (i.e., kernel size 3×3 and stride of 1 and padding of 1) and dilated convolution (i.e., kernel size 3×3 , stride of 1, padding of 2 and dilation rate of 2), each convolution is with a batch normalization layer. Obviously, three different convolution output size are the same. And we concatenate the feature maps of three different convolution outputs before a ReLU activation and vote to select valuable features by another pointwise convolution:

$$f_{concat} = \sigma_2(\text{Concat}\{\text{BN}\{\text{PointwiseConv}(f)\}, \text{BN}\{\text{OrdinaryConv}(f)\}, \text{BN}\{\text{DilationConv}(f)\}\}) \quad (3)$$

$$f_s = f \times \sigma_3(\text{PointwiseConv}(f_{concat})) + f \quad (4)$$

Where f represents encoding feature, σ_2 and σ_3 represents the ReLU and Sigmoid activation, f_{concat} represents the concatenate feature, f_s represents the output feature from multi-scale attention gate to be spliced with the decoder.

3. DATASET AND EXPERIMENT DETAILS

We pick Breast UltraSound Images (BUSI) [4] and private Thyroid UltraSound dataset (TUS) to evaluate our results. BUSI collected 780 breast ultrasound images, including normal, benign and malignant cases of breast cancer with their corresponding segmentation results. We only used benign and malignant images (647 images). TUS is collected from the

Ultrasound Department of the Affiliated Hospital of Qingdao University. It includes 192 cases, totally 1942 thyroid ultrasound images with segmentation results by three experienced radiologists.

We use the Pytorch to implement the CMU-Net and adopt the same training process as UNeXt [6]. The combination of binary cross entropy (BCE) and dice loss (Dice) is used. The loss L between the predicted map \hat{y} and ground truth target map y is formulated as:

$$L = 0.5BCE(\hat{y}, y) + Dice(\hat{y}, y) \quad (5)$$

The experiments use Adam optimizer to optimize the network. We set the initial learning rate to 0.0001 and momentum is 0.9. We also set the batch size to 8 and total training for 300 epochs.

In data processing, the two datasets are randomly split thrice, 80% for training and 20% for validation. In addition, we resize all the images 256×256 and perform random rotation and flip for data augmentation.

4. RESULTS AND DISCUSSION

We compare CMU-Net with most of U-Net based models like U-Net [2], U-Net++ [3], Attention U-Net [4], U-Net3+ [5], TransUnet [8] and UNeXt [6]. Note that the encoder of U-Net++ is ResNet34 [15]. Moreover, we carry out a lot of experiments with different ConvMixer depths and kernel sizes and finally the ConvMixer block with a depth of 7 ($L=7$) and a kernel size of 7 ($k=7$) can achieve the best performance.

Table 1. Compare our method with most of U-Net based models on the BUSI (%)

	IOU	Recall	Precision	F1	Accuracy
U-Net[2]	68.49 \pm 0.18	80.57 \pm 2.24	82.52 \pm 2.34	80.88 \pm 0.07	96.74 \pm 0.08
Attention U-Net[4]	70.38 \pm 1.48	81.44 \pm 1.67	83.66 \pm 0.61	82.16 \pm 0.97	96.99 \pm 0.12
U-Net++[3]	69.49 \pm 0.15	81.27 \pm 1.36	81.87 \pm 1.07	81.15 \pm 1.25	96.34 \pm 0.22
U-Net3+[5]	65.39 \pm 0.12	77.54 \pm 2.02	80.66 \pm 2.50	78.22 \pm 0.07	95.96 \pm 0.09
TransUnet[8]	66.75 \pm 1.50	78.65 \pm 4.32	81.33 \pm 2.71	79.46 \pm 1.05	96.24 \pm 0.38
UNeXt[6]	66.76 \pm 0.05	77.25 \pm 1.43	83.49 \pm 1.28	79.72 \pm 0.12	96.60 \pm 0.05
CMU-Net	73.27\pm0.43	84.26\pm0.54	84.81\pm1.32	84.16\pm0.47	97.33\pm0.14

Table 2. Compare our method with most of U-Net based models on our private TUS (%)

	IOU	Recall	Precision	F1	Accuracy
U-Net[2]	83.51 \pm 0.10	90.15 \pm 0.91	92.00 \pm 0.83	90.97 \pm 0.05	99.21 \pm 0.01
Attention U-Net[4]	83.90 \pm 0.14	90.87 \pm 0.58	91.71 \pm 0.41	91.21 \pm 0.08	99.22 \pm 0.01
U-Net++[3]	84.23 \pm 0.33	90.59 \pm 0.35	92.34 \pm 0.32	91.40 \pm 0.20	99.22 \pm 0.03
U-Net3+[5]	83.60 \pm 0.14	90.21 \pm 0.90	92.02 \pm 0.78	91.01 \pm 0.07	99.18 \pm 0.01
TransUnet[8]	82.75 \pm 0.25	89.51 \pm 0.19	91.66 \pm 0.23	90.47 \pm 0.13	99.13 \pm 0.02
UNeXt[6]	81.19 \pm 0.18	88.41 \pm 1.13	90.86 \pm 1.17	89.50 \pm 0.07	99.05 \pm 0.02
CMU-Net	84.75\pm0.30	91.53\pm0.37	92.02\pm0.13	91.71\pm0.17	99.27\pm0.01

Furthermore, we adopt five commonly used metrics to quantitatively compare the performance of different segmentation models: IOU, Recall, Precision, F1-value and Accuracy. We report the mean and variance of the BUSI and TUS validation sets in Table 1 and Table 2.

As shown in Table 1 and Table 2, CMU-Net obtains better segmentation performance than all the baselines. Especially, on the BUSI, CMU-Net achieves the highest performance and improves at least 2.89% in IOU and 2.00% in F1 values metrics. And Attention U-Net is second, which proves that the attention gates could improve the performance. Further for TUS, the CMU-Net almost improves every metrics compared with other models and achieves a better trade-off between recall and specificity. The TransUnet, which consists of hybrid CNN and Transformer structures, needs to feed a large amount of training data, performs unsatisfactorily on small datasets. On the contrary, CMU-Net demonstrates its advantages with consideration to both local and global information, and highlight features that are meaningful for the task. Some results are shown in Figure 4. It can be seen that CMU-Net gives more accurate outputs with more precise spatial location and shape.

Moreover, we conducted an ablation study to analyze the contribution of each module in the CMU-Net. As shown in Table 3, we can see that the performance of the original U-

Net has been greatly improved after the introduction of the ConvMixer block, which shows that the ConvMixer block can effectively mix remote spatial locations to enable the network to learn valuable global context information. Next, we add multi-scale attention gates to improve the performance further, it shows multi-scale attention gates can effectively magnify the affection of helpful encoder features in knowledge transfer.

5. CONCLUSION AND PERSPECTIVES

In this work, we have proposed a strong full convolutional network CMU-Net for medical ultrasound segmentation. We introduce ConvMixer block in U-shape architecture to build a strong encoder for obtain global content information and propose a multi-scale attention gate for emphasizing valuable features to achieve efficient skip connections. We validated CMU-Net on multiple ultrasound datasets and achieved excellent performance. In the future, more experiments can be carried out on CMU-Net, such as using larger convolution kernels, placing ConvMixer blocks at different encoder levels. Further analyzing error result to improve the accuracy. Combining with the physiological and anatomical structures of the lesions to improve the interpretability of the model.

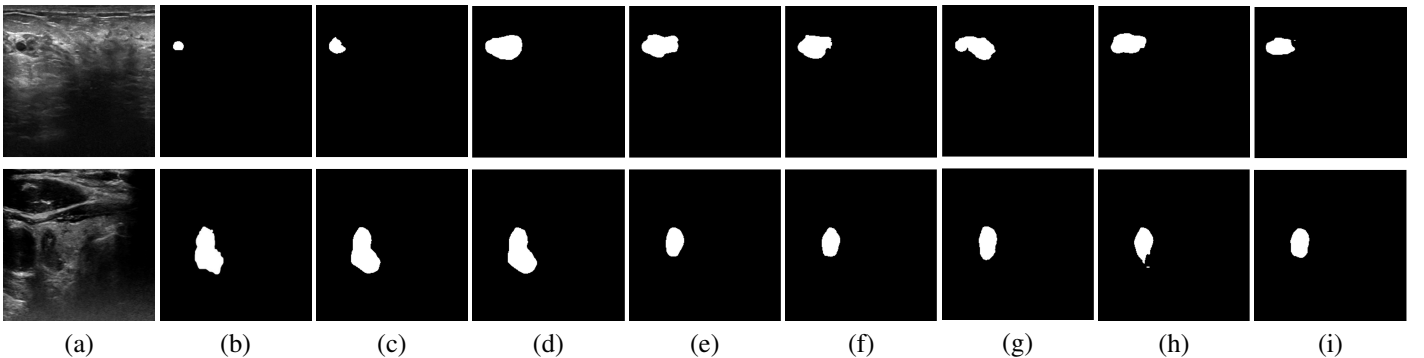


Fig. 4. Segmentation result. Row 1 - BUSI dataset, Row 2 - TUS dataset. (a) Input and (b) Ground Truth. Predictions of (c) CMU-Net (d) Attention U-Net (e) TransUnet (f) U-Net (g) U-Net++ (h) U-Net3+ and (i) UNeXt.

Table 3. Ablation Study on the BUSI

	IOU	F1	Accuracy
Original U-Net	68.49 \pm 0.18	80.88 \pm 0.07	96.74 \pm 0.08
U-Net + ConvMixer	72.36 \pm 0.37	83.57 \pm 0.30	97.23 \pm 0.04
U-Net + ConvMixer + Multi-scale attention gate	73.27 \pm 0.43	84.16 \pm 0.47	97.33 \pm 0.14

6. COMPLIANCE WITH ETHICAL STANDARDS

Informed consent was obtained from all individual participants involved in the study.

7. ACKNOWLEDGMENTS

This work is supported, in part, by Shandong Natural Science Foundation of China; the Grant numbers is ZR2020MH290.

8. REFERENCES

- [1] Qinghua Huang, Fan Zhang, and Xuelong Li, “Machine learning in ultrasound computer-aided diagnostic systems: a survey,” *BioMed research international*, vol. 2018, 2018.
- [2] Olaf Ronneberger, Philipp Fischer, and Thomas Brox, “U-net: Convolutional networks for biomedical image segmentation,” in *International Conference on Medical image computing and computer-assisted intervention*. Springer, 2015, pp. 234–241.
- [3] Zongwei Zhou, Md Mahfuzur Rahman Siddiquee, Nima Tajbakhsh, and Jianming Liang, “Unet++: A nested u-net architecture for medical image segmentation,” in *Deep learning in medical image analysis and multimodal learning for clinical decision support*, pp. 3–11. Springer, 2018.
- [4] Ozan Oktay, Jo Schlemper, Loic Le Folgoc, Matthew Lee, Mattias Heinrich, Kazunari Misawa, Kensaku Mori, Steven McDonagh, Nils Y Hammerla, Bernhard Kainz, et al., “Attention u-net: Learning where to look for the pancreas,” *arXiv preprint arXiv:1804.03999*, 2018.
- [5] Huimin Huang, Lanfen Lin, Ruofeng Tong, Hongjie Hu, Qiaowei Zhang, Yutaro Iwamoto, Xianhua Han, Yen-Wei Chen, and Jian Wu, “Unet 3+: A full-scale connected unet for medical image segmentation,” in *ICASSP 2020-2020 IEEE International Conference on Acoustics, Speech and Signal Processing (ICASSP)*. IEEE, 2020, pp. 1055–1059.
- [6] Jeya Maria Jose Valanarasu and Vishal M Patel, “Unext: Mlp-based rapid medical image segmentation network,” *arXiv preprint arXiv:2203.04967*, 2022.
- [7] Ashish Vaswani, Noam Shazeer, Niki Parmar, Jakob Uszkoreit, Llion Jones, Aidan N Gomez, Łukasz Kaiser, and Illia Polosukhin, “Attention is all you need,” *Advances in neural information processing systems*, vol. 30, 2017.
- [8] Jieneng Chen, Yongyi Lu, Qihang Yu, Xiangde Luo, Ehsan Adeli, Yan Wang, Le Lu, Alan L Yuille, and Yuyin Zhou, “Transunet: Transformers make strong encoders for medical image segmentation,” *arXiv preprint arXiv:2102.04306*, 2021.
- [9] Jeya Maria Jose Valanarasu, Poojan Oza, Ilker Hacıhaliloglu, and Vishal M Patel, “Medical transformer: Gated axial-attention for medical image segmentation,” in *International Conference on Medical Image Computing and Computer-Assisted Intervention*. Springer, 2021, pp. 36–46.
- [10] Wenxuan Wang, Chen Chen, Meng Ding, Hong Yu, Sen Zha, and Jiangyun Li, “Transbts: Multimodal brain tumor segmentation using transformer,” in *International Conference on Medical Image Computing and Computer-Assisted Intervention*. Springer, 2021, pp. 109–119.
- [11] Alexey Dosovitskiy, Lucas Beyer, Alexander Kolesnikov, Dirk Weissenborn, Xiaohua Zhai, Thomas Unterthiner, Mostafa Dehghani, Matthias Minderer, Georg Heigold, Sylvain Gelly, et al., “An image is worth 16x16 words: Transformers for image recognition at scale,” *arXiv preprint arXiv:2010.11929*, 2020.
- [12] Asher Trockman and J Zico Kolter, “Patches are all you need?,” *arXiv preprint arXiv:2201.09792*, 2022.
- [13] Walid Al-Dhabyani, Mohammed Gomaa, Hussien Khaled, and Aly Fahmy, “Dataset of breast ultrasound images,” *Data in brief*, vol. 28, pp. 104863, 2020.
- [14] Dan Hendrycks and Kevin Gimpel, “Gaussian error linear units (gelus),” *arXiv preprint arXiv:1606.08415*, 2016.
- [15] Kaiming He, Xiangyu Zhang, Shaoqing Ren, and Jian Sun, “Deep residual learning for image recognition,” in *Proceedings of the IEEE conference on computer vision and pattern recognition*, 2016, pp. 770–778.